RSC Advances

PAPER

View Article Online
View Journal | View Issue

Cite this: *RSC Adv.*, 2014, **4**, 44700

Adsorption of polyethylenimine and its interaction with a genomic DNA on a silicon oxynitride surface characterized by dual polarization interferometry

Huaguo Xu,[a] Fujian Huang*[a] and Haojun Liang*[ab]

Received 17th June 2014
Accepted 10th September 2014

DOI: 10.1039/c4ra05840b

www.rsc.org/advances

Dual polarization interferometry was used to investigate the adsorption of polyethylenimine (PEI) on a silicon oxynitride chip surface, as well as to study the subsequent interaction between PEI and a genomic DNA. A compact homogeneous PEI layer formed initially as a result of their strong electrostatic attraction to the negatively charged chip surface. With the adsorption going on, a short time adsorption process with constant speed was observed and the subsequent PEI molecules loosely attached on the chip surface because of the electrostatic repulsion and crowded surface conditions. A loose and thick DNA layer formed on the PEI surface due to its rigidity. Further PEI deposition induced DNA conformation changes and the swelling of the PEI–DNA complex layer, which resulted in a dramatic layer thickness increase. Under high PEI concentration, the layer mass and thickness increments were partially lost as DNA was stripped off by PEI molecules. This result was interpreted in terms of overcharged DNA–PEI complex formation and the strong electrostatic repulsion between the first PEI layer and the newly formed overcharged DNA–PEI complexes. The explanation was proved by the case of the assembly process in PBS. No stripping effect was found even at a high PEI concentration in PBS because of the salt screening effect and the low charge density of PEI.

Introduction

Polyelectrolyte multilayers (PEMs) are an interesting class of material which can be used for drug delivery,[1,2] enhanced gene transfection[3,4] and other new biomedical applications such as tissue engineering.[5] To construct functional and organized ultrathin multilayer biomacromolecule-containing films in predetermined ways is an important area of research in biochemistry and biotechnology.[6] The layer-by-layer assembly (LbL) technique, which was developed by Decher *et al.*,[7–9] is one of the most perspective methods for thin films fabrication. The first step of layer-by-layer assembly process is to use one kind of polyelectrolyte coating the surface, and then different polyelectrolytes were deposited on the surface alternately through ion-pair formation,[10,11] internal diffusion and interpenetration.[12,13] Different assembly systems, because of their distinct interaction manners, show different growth styles.[14–18]

The polyelectrolytes selected for this study were PEI and calf thymus DNA. PEI, which is usually used in gene transfection, is a positively charged polyamine.[19–22] PEI thin film coating is a critical technology which can be used to immobilize DNA on the surface to fabrication of biosensors and gene chips *via* interfacial adsorption. Double-stranded DNA is a highly negatively charged rigid biomacromolecule with a persistence length of ~50 nm.[23] The interactions between DNA and multivalent cations can induce conformational changes, condensation, and aggregation of DNA chains in solution, forming globule-like complexes.[24] PEI is a type of polycation that can also induce the formation of globule-like complexes. The interaction process between PEI and DNA in the solution is controlled by salt conditions and by the positively charged density of polycations.[25,26] Highly positively charged densities of polycations yield globular, overcharged polycation/DNA aggregates.[27]

Several studies have extensively investigated the interaction between DNA and PEI, as well as the charge and conformation of PEI–DNA complexes in solution. However, the interaction process, especially the conformation information of PEI–DNA complexes during the interaction process on a solid–liquid interface, is not yet clearly understood. Whether the formation of this overcharged complex will affect the interaction process of PEI and DNA on a planar surface has yet to be revealed. The assembly process of PEI and DNA on a planar surface was monitored using DPI equipment for the first time to solve the puzzle.

[a]*CAS Key Laboratory of Soft Matter Chemistry, Department of Polymer Science and Engineering, University of Science and Technology of China, Hefei, Anhui 230026, People's Republic of China. E-mail: hjliang@ustc.edu.cn; fjhuang@ustc.edu.cn; Fax: +86-551-3607824; Tel: +86-551-3607824*

[b]*Hefei National Laboratory for Physical Sciences at Microscale, University of Science and Technology of China, Hefei, Anhui 230026, People's Republic of China*

Experimental

Materials and sample preparation

DNA sodium salt from calf thymus type I and aqueous PEI (M_w = 750 000) 50% (w/v) solution were purchased from Sigma Chemical Co. Aqueous PEI (M_w = 70 000) 30% (w/v) solution was obtained from Alfa Co. Other agents used were of analytical grade or higher. The water used was of Milli-Q grade (Millipore). The PBS (pH 7.4) was prepared with 10 mM NaH_2PO_4–Na_2HPO_4 and 137 mM NaCl. Water and buffer were degassed before use. The aqueous and PBS solutions of DNA were prepared at 100 μg mL^{-1} independently using ultrapure water and PBS. PEI solutions with different concentrations were prepared using water or PBS. The aqueous DNA solution was dialyzed against ultrapure water overnight before use to reduce the effect of salinity.

Collector surface

Silicon oxynitride chip was used during the DPI experiments. The bare sensor chip, FB 80 Unmodified (Farfield Sensors) was first cleaned with 2% (w/v) Hellmanex solution (Hellma GmbH & Co.) for 30 min, and then incubated in a hot piranha solution (H_2O_2/H_2SO_4, 3 : 7, v/v) for 30 min. (**Caution**: "Piranha" solution reacts violently with organic materials; it must be handled with extreme care.) Afterward, the chip was fully rinsed with ultrapure water and blown dry with nitrogen. The chip surface is composed of hydrophilic and negatively charged silicon hydroxyl.

Dual polarization interferometry experiments

PEI adsorption, DNA immobilization, and further interaction between PEI and DNA were investigated real-time using DPI (AnaLight Bio200, Farfield Group, Ltd., Crewe, United Kingdom). The details of the instrument and theory have been described in previous studies.[28–30] The instrument works with a laser emitting light at 632.8 nm. The polarization state of the light was switched between transverse electric (TE) and transverse magnetic (TM) using a polarizer at 50 Hz. The fluidic system coupled to the instrument consisted of a high-performance liquid chromatography injector valve and an external pump (Harvard Apparatus, PHD2000), which provides a controlled continuous fluid flow over two channels on the chip surface. The DPI experiment was performed at 20 °C ± 0.002 °C in a temperature-controlled enclosure that maintains thermal stability to within 1 mK using an unmodified chip in ultrapure water and PBS. Before the experiment, the sensor chip and PBS were calibrated using 80% (w/w) ethanol/water solution and ultrapure water. The refractive indexes (RIs) of the ethanol/water solution and ultrapure water are known. Therefore, the waveguide thickness, RI, and RI of PBS were calibrated.

After calibration, the flow rate was changed to 25 μL min^{-1}. A PEI solution (1.5 mg mL^{-1}; M_w = 70 000, 750 000) was injected over both channels for 6 min before returning to water or PBS. After a steady baseline was reached, a DNA (100 μg mL^{-1}) solution was injected over both channels for 6 min at a flow rate of 25 μL min^{-1} before returning to water or PBS. Aqueous PEI (M_w = 70 000) solutions in the range of 100 μg mL^{-1} to 1000 μg mL^{-1}, PEI (1500 μg mL^{-1}; M_w = 750 000) aqueous solution, PEI (1000 μg mL^{-1}; M_w = 70 000) PBS solution, were injected over both channels for 6 min to investigate the interactions.

The phase changes in the TE and TM modes were investigated real-time. The absolute thickness and RI were resolved directly using the TM and TE phase values through analysis software. The adsorbed mass was quantified according to De Feijter's equations:[31]

$$\rho_L = \frac{n_L - n_{buffer}}{dn/dc} \quad (1)$$

$$m_L = \rho_L \tau_L \quad (2)$$

where m_L is the layer of mass per unit area (ng mm^{-2}), τ_L is the layer thickness (nm); n_L and n_{buffer} are the refractive indexes of the layer and the bulk solution, respectively, and dn/dc is the RI increment (cm^3 g^{-1}). A dn/dc value of 0.175 was used according to Lee *et al.*,[32] although we note that the experimental conditions in our experiments were not the same as those employed by Lee *et al.*; therefore, this value was merely an estimate. The thickness and RI were measured parameters; the constant dn/dc was used to calculate the layer mass and density. Although the values reported for the density and mass might not be absolute, the trends reported herein should be accurate.

According to the calculated parameters described in the preceding text, conclusions can be made regarding the adsorption of PEI and the interaction mechanism of giant genomic DNA with PEI on silicon oxynitride chip surface.

Results and discussion

Adsorption of PEI on silica oxynitride chip surface

In order to immobilize DNA on chip surface and then study the interaction between DNA and PEI, a PEI layer was first fabricated on silica oxynitride chip surface. As silica oxynitride chip surface was negatively charged in both pure water and PBS, the positively charged PEI can be successfully adsorbed on the chip surface through electrostatic interaction. Fig. 1 shows the real-time mass change during the adsorption of PEI on the chip surface. As can be seen, the adsorption process is very fast. At

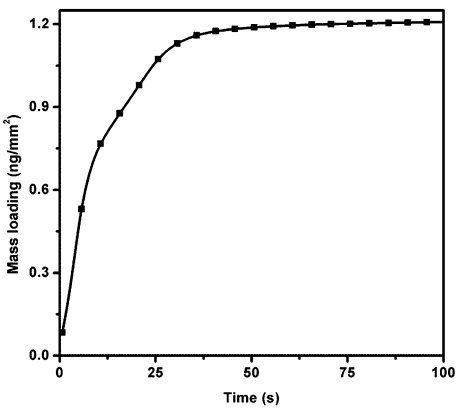

Fig. 1 Real-time DPI measurement of mass during the adsorption of PEI (M_w = 750 000) on silica chip surface in pure water.

the onset of the adsorption, the mass increased quickly because of the strong electrostatic interaction between PEI and chip surface. With the adsorption going on, the mass increased slowly and quickly plateaued.

Mass loading rate dm_L/dt was plotted against mass loading m_L to better understand the whole adsorption process (Fig. 2). At the beginning of the adsorption, the mass loading rate increased to the maximum. This first time increase of mass loading rate is attributed to the concentration increase of the PEI solution over the chip surface. Before the injection of PEI solution, the micro-fluidic flow chamber was full of pure water. When the PEI solution reached the chamber, it took a few seconds to introduce the solution over the entire chip surface. Thus, the concentration over the chip surface changed from 0 to maximum, and then kept stable in the following adsorption process. This concentration increase caused the first increase of mass loading rate. With continuous adsorption, more PEI molecules occupied the surface, and so the mass loading rate decreased. Interestingly, a short time adsorption process with constant speed was observed when the mass loading reached about 0.8 ng mm^{-2}. From this point the adsorption process was controlled by the diffusion process of PEI molecules from solution to the chip surface, that is, at this stage the transport from the bulk is the rate-determining step. With the adsorption going on, the chip surface was so crowded that the mass loading rate decreased again until the adsorption process stopped.

Two different slopes were observed after we plotted the layer thickness change against the mass loading (Fig. 3). The result indicates an initial flat conformation followed by a steep increase in layer thickness. PEI was first adsorbed on the chip surface as a homogeneous compact layer. Heterogeneous layer formed as more PEI molecules diffused to the interface. At the break in the slope (0.8 ng mm^{-2}), the chip surface was so crowded that the following PEI molecules can only attach partly onto the surface, resulting in the steep increase in slope and the formation of a diffuse outer layer as demonstrated in previous study.[33]

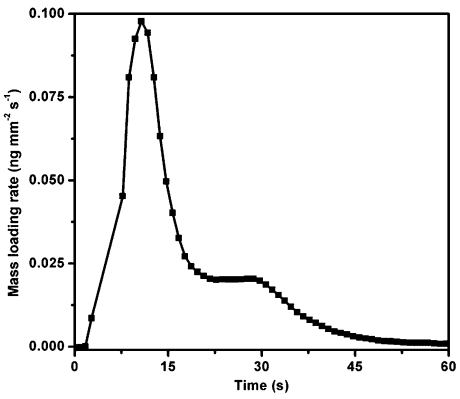

Fig. 2 Changes in the mass loading rate during the adsorption of PEI on silica chip surface.

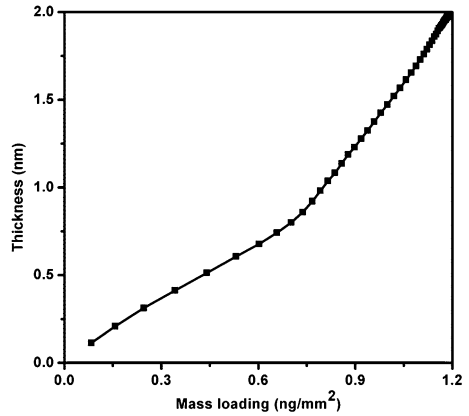

Fig. 3 Changes in the layer thickness as function of the mass loading of PEI on silica chip surface during the initial stage of adsorption.

Immobilization of DNA on preadsorbed PEI surface

After the adsorption of PEI on chip surface, a DNA solution was injected over preadsorbed PEI surface. DNA was electrostatically immobilized on the preadsorbed PEI surface to form a relatively compact layer. Fig. 4 shows the real-time mass, thickness, and RI (density) changes during the adsorption of PEI, immobilization of DNA and subsequent interaction between PEI and preimmobilized DNA. Upon the injection of DNA solution through the preadsorbed (marked "DNA injection" in Fig. 4), the mass and thickness increased quickly accompanied with the decrease of the layer density (RI). The increasing thickness

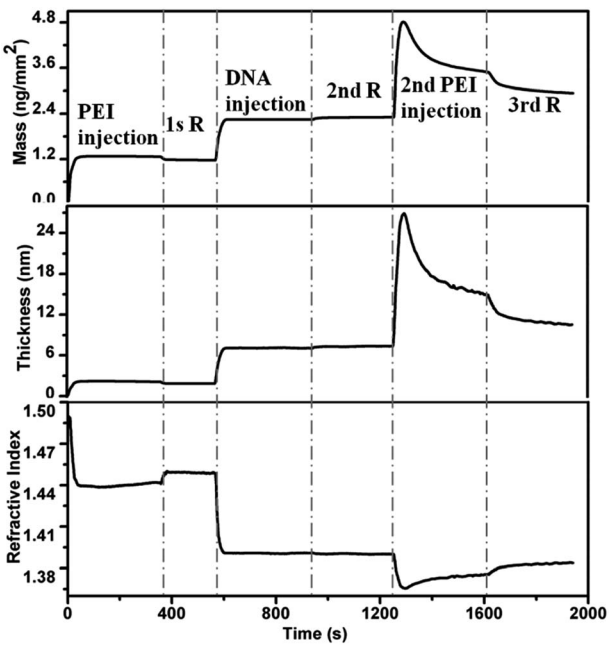

Fig. 4 Real-time DPI measurements of mass, thickness and RI during the first three layers assembly process of PEI (M_w = 750 000) and DNA on silicon chip surface in pure water. The first PEI injection occurs at t = 0 s and the subsequent five steps are labelled according to the first rinse "1st R", DNA injection, second rinse "2nd R", second PEI addition "2nd PEI injection", and third rinse "3rd R".

with decreasing RI observed during the course of the mass loading suggests that a looser and thicker DNA layer formed due to its rigidity. A 5.5 nm DNA layer was observed in this study, which is different with the previously reported 14.3 nm DNA layer formation on a PEI surface in PBS.[34] The difference may be due to the dissimilar experimental environment of the previous[34] and present study. Our observation involved pure water, in which DNA chains can be fully negatively charged. Such chains may adopt a more extended conformation (thin layer) relative to the ones in the PBS.

Interaction between PEI and preimmobilized DNA in pure water

In order to investigate the interaction between PEI and preimmobilized DNA, a PEI solution (1.5 mg mL^{-1}) was injected over formed PEI–DNA bilayer. Fig. 4 ("2nd PEI injection") shows the real-time mass, thickness, and RI (density) changes upon the injection of PEI. As can be seen, the interaction between PEI and preimmobilized DNA was a very quick process in which the mass and thickness reached the maximum of 4.8 ng mm^{-2} and 27 nm in 10 s, while the RI decreased significantly. After that, the layer mass and thickness decreased dramatically accompanied with RI increasing. The decreases in layer thickness and mass suggest that some of the preimmobilized DNA molecules were stripped off upon the injection of PEI through PEI–DNA bilayer. In solution, PEI can interact with DNA through electrostatic interaction, making the DNA condense and forming overcharged PEI–DNA complex. In the case of interaction on surface, the interaction between PEI and preadsorbed DNA made the DNA conformation change and the formed PEI–DNA bilayer swell, resulting in the drastic increase in layer thickness. The electrostatic repulsion between the first PEI layer and the newly formed overcharged DNA–PEI complexes made the preimmobilized DNA strip off in the form of PEI–DNA complexes, resulting in the subsequent decreases of layer thickness and mass.

To a deep insight of the interaction between PEI and preimmobilized DNA, five parallel experiments with respective 100, 300, 500, 800 and 1000 μg mL^{-1} of PEI solutions were performed to understand their concentration dependency. The variation of mass, thickness and RI with time were then recorded upon the injection of PEI solution with corresponding concentration through preimmobilized DNA layer. Fig. 5 shows the real-time changes of mass, thickness, and RI of the layers upon the injections of PEI solutions ranging from 100 μg mL^{-1} to 1000 μg mL^{-1}. At low concentrations, the mass and thickness of the layers increase with the increasing of PEI concentration, which mean more PEI molecules were adsorbed onto the layer in concentrated solutions. The drop of RIs' value corresponding to the concentrated solutions is the signal of loosing parking of PEI chains on the surface. This can be attributed to the swollen of DNA–PEI complex layer due to the penetration of the PEI chains into the PEI–DNA bilayer. When the PEI concentration increases to 800 μg mL^{-1}, the mass and thickness increments relied on addition of the PEI begin to be partially lost on exposure to the PEI solution, as DNA is stripped off by its oppositely charged partner. This striping effect is more dramatic at the PEI concentration of 1000 μg mL^{-1}.

Variations in the thickness of the layer were plotted against surface excesses to more clearly understand the whole interaction process (Fig. 6). As can be seen, the variations in thickness with mass densities in sets with lower concentrations (100, 300, 500, and 800 μg mL^{-1}) are located in an identical line, whereas the curve corresponding to high concentration (1000 μg mL^{-1}) deviates upward. These findings imply that the interaction processes in the two systems are governed by different interaction styles. If the macromolecules just simply attach on the preformed layer surface, each individual macromolecule chain generally offers its own contribution to the thickness of the layer. The thickness will then essentially grow linearly with the number of chains involved in the layer. If the adsorbed chains interact (the chains repulse one another or make the chain conformation change), the growth of the thickness may deviate from the linearity. According to previous studies, PEI interacts with DNA by electrostatic attraction and embedding in the base pair, forming an overcharged globule-like DNA–PEI complex in solution.[35] For surface interactions, electrostatic attraction and embedding in the base pair induce conformational changes to the DNA layer, resulting in the swelling of the layer. In the curve corresponding to 1000 μg mL^{-1} concentration, thickness was observed to grow exponentially with mass. This process is caused by the electrostatic repulsion between newly formed overcharged DNA–PEI complexes and the PEI chains.

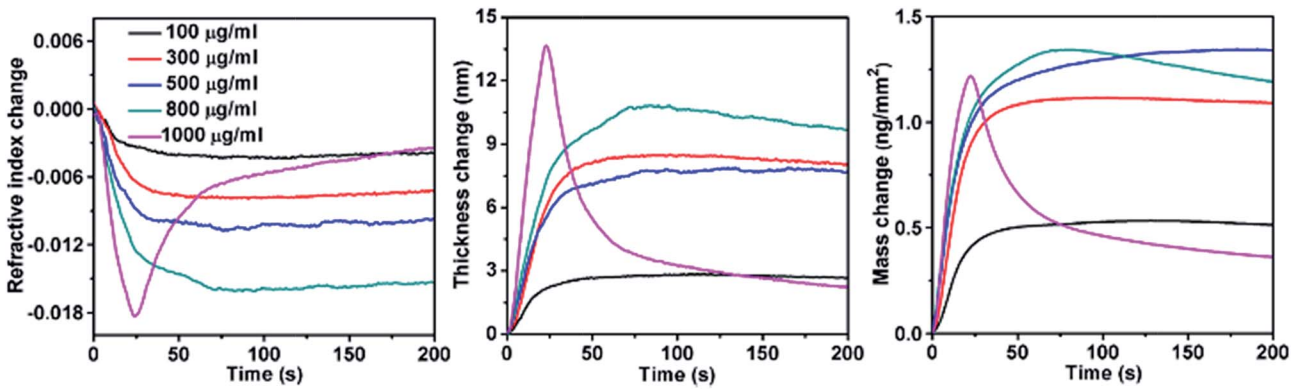

Fig. 5 Changes in the RI, thickness and mass of the PEI–DNA bilayer as a function of PEI (M_w = 70 000) with different concentration injections.

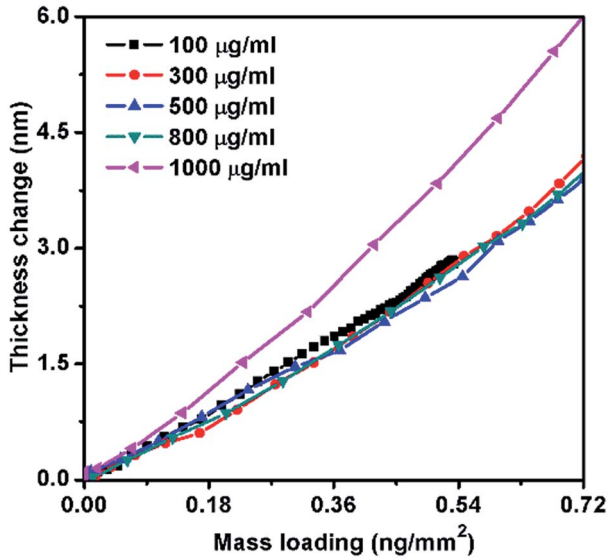

Fig. 6 Changes in the layer thickness as functions of the mass loading of the PEI (M_w = 70 000) third layer with different concentrations during the initial stage of each adsorption from Fig. 5.

At lower PEI concentrations, relatively less numbers of PEI chains exist near the second DNA surface and the layer is in a starving state. Thus, the chains near the surface were quickly adsorbed onto the layer. The adsorption process in the starving state is governed by the PEI concentration near the surface. Therefore, the adsorbed chains are permitted to have relatively longer periods to diffuse. The adsorbed chains may distribute homogeneously within the layer to guarantee the separation of chains at a greater distance to avoid the higher energy penalty induced by the strong electrostatic repulsion. However, in systems with higher concentrations, the adsorption is governed by diffusion and a non-equilibrium process because the chains near the surface are abundant. The PEI chains adsorbed on the layer do not have enough time to organize conformation; thus, the separation of chains at a greater distance to allow the system to reach global minima is not guaranteed. As a result, chains will repulse other chains in proximity. Two contributions were made to the growth of layer thickness. One is from the number of PEI chains, and the other is from the repulsion of chains. These two contributions make the plot corresponding to the 1000 μg mL^{-1} follow an exponential-like manner and deviate upward from linearity.

Interaction between PEI and preimmobilized DNA in PBS

A similar experiment was performed in PBS under a high PEI concentration to confirm the striping mechanism of the DNA from the surface discussed above. The DNA was immobilized on a pre-adsorbed PEI surface. Thereafter, a PEI solution at 1000 μg mL^{-1} was injected over the PEI–DNA bilayer surface in PBS. Fig. 7 shows the real-time changes in mass, thickness, density, and RI of the PEI–DNA bilayer upon the injection of PEI solution in PBS. The swelling of the DNA layer in the PBS was also observed after the deposition of PEI on the surface. However, the swelling was not as dramatic as that in pure water, and no striping was observed. The interaction of DNA and PEI in PBS differs slightly from that in pure water. In the PBS (pH 7.4), PEI is less protonated compared with that in pure water (pH 5), which reduces the positive charge density of PEI.[36] On the other hand, salt in the PBS can screen charges, thus reducing the repulsion between identical charges. The salt screening effect and the lesser protonation of PEI contribute relatively small mass loads on the DNA layer compared with that in pure water under the same PEI concentration. A small PEI mass loading can reduce the positive charge of newly formed DNA–PEI complexes. This low positive charge together with the salt screening effect reduces the repulsion force between the formed DNA–PEI complex and the positively charged PEI surface, thus preventing the striping phenomenon.

As the adsorption mass reaches the plateau point and stabilizes, the layer becomes thinner, accompanied by an increase in layer density (Fig. 7). In PBS, PEI and DNA are surrounded by counter-ions. Once the PEI solution reached the DNA surface, a rapid rise in thickness and mass goes with a sharp decrease in average film RI, which is similar with that in pure water. The difference is that, mass decreases slightly accompanied by the significant thickness decrease and the density (RI) increase till a relatively stable state was achieved during the following adsorption. During the interaction process, PEI quickly attached on the DNA surface which made DNA conformational change. After that,

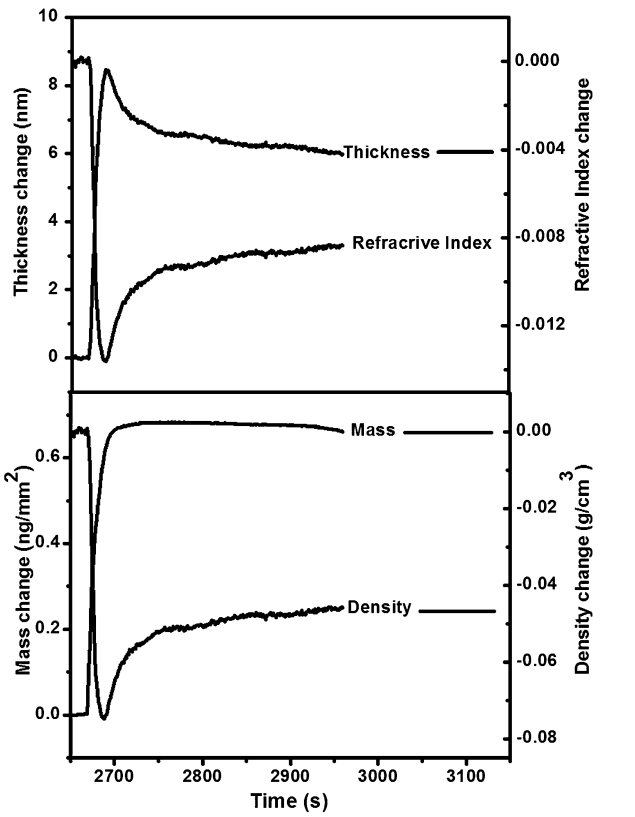

Fig. 7 Real-time DPI measurements of thickness, mass, RI, and density changes during the injection of PEI (M_w = 70 000) over the PEI–DNA bilayer surface in the PBS. Here, the PEI concentration was 1000 μg mL^{-1}.

some counter-ions were eliminated as the polymers rearranged themselves and slowly interacted with each other more strongly.

Conclusions

The adsorption of PEI and the interaction between PEI and DNA on silicon oxynitride chip surface were evaluated real time using dual polarization interferometry. The overall results show that the PEI adsorption process exhibited multiphasic adsorption behavior. A compact homogeneous PEI layer formed at the beginning of adsorption. With the adsorption going on, a short time adsorption process with constant speed was observed and the subsequent PEI chain can just loosely attach on the chip surface because of the crowded surface condition. For the interaction between DNA and PEI on surface, we found that when PEI injected over PEI–DNA complex bilayer, DNA can be stripped off under high PEI concentration. We prove that the stripping results from the formation of overcharged DNA–PEI complex and the strong electrostatic repulsion between first PEI layer and overcharged DNA–PEI complex, which means that under appropriate salt condition the stripping can be avoided because of the charge shielding effect. This study resolves a new interaction process of highly negative charged DNA with polycation and provides useful information for fabrication of biosensors and gene chips *via* interfacial adsorption.

Acknowledgements

We thank the National Natural Science Foundation of China (91127046), the National Basic Research Program of China (2012CB821500), the Fundamental Research Funds for the Central Universities (WK2060200013), and the Financial Grant from the China Postdoctoral Science Foundation (2014M551808) for their financial support.

Notes and references

1 B. M. Wohl and J. F. J. Engbersen, *J. Controlled Release*, 2012, **158**, 2–14.
2 S. De Koker, R. Hoogenboom and B. G. De Geest, *Chem. Soc. Rev.*, 2012, **41**, 2867–2884.
3 A. S. Qi, P. Chan, J. Ho, A. Rajapaksa, J. Friend and L. L. Yeo, *ACS Nano*, 2011, **5**, 9583–9591.
4 J. H. Ke and T. H. Young, *Biomaterials*, 2010, **31**, 9366–9372.
5 T. Boudou, T. Crouzier, K. F. Ren, G. Blin and C. Picart, *Adv. Mater.*, 2010, **22**, 441–467.
6 R. J. Pei, X. Q. Cui, X. R. Yang and E. K. Wang, *Biomacromolecules*, 2001, **2**, 463–468.
7 G. Decher, *Science*, 1997, **277**, 1232–1237.
8 N. Jessel, F. Atalar, P. Lavalle, J. Mutterer, G. Decher, P. Schaaf, J. C. Voegel and J. Ogier, *Adv. Mater.*, 2003, **15**, 692–695.
9 N. Benkirane-Jessel, P. Lavalle, F. Meyer, F. Audouin, B. Frisch, P. Schaaf, J. Ogier, G. Decher and J. C. Voegel, *Adv. Mater.*, 2004, **16**, 1507–1511.
10 G. Decher, J. D. Hong and J. Schmitt, *Thin Solid Films*, 1992, **210**, 831–835.
11 K. Lowack and C. A. Helm, *Macromolecules*, 1998, **31**, 823–833.
12 M. Raposo, R. S. Pontes, L. H. C. Mattoso and O. N. Oliveira, *Macromolecules*, 1997, **30**, 6095–6101.
13 N. C. de Souza, J. R. Silva, R. Di Thommazo, M. Raposo, D. T. Balogh, J. A. Giacometti and O. N. Oliveira, *J. Phys. Chem. B*, 2004, **108**, 13599–13606.
14 M. Schonhoff, *Curr. Opin. Colloid Interface Sci.*, 2003, **8**, 86–95.
15 G. Decher, M. Eckle, J. Schmitt and B. Struth, *Curr. Opin. Colloid Interface Sci.*, 1998, **3**, 32–39.
16 D. L. Elbert, C. B. Herbert and J. A. Hubbell, *Langmuir*, 1999, **15**, 5355–5362.
17 F. Boulmedais, V. Ball, P. Schwinte, B. Frisch, P. Schaaf and J. C. Voegel, *Langmuir*, 2003, **19**, 440–445.
18 C. Picart, P. Lavalle, P. Hubert, F. J. G. Cuisinier, G. Decher, P. Schaaf and J. C. Voegel, *Langmuir*, 2001, **17**, 7414–7424.
19 C. G. Koh, X. H. Kang, Y. B. Xie, Z. Z. Fei, J. J. Guan, B. Yu, X. L. Zhang and L. J. Lee, *Mol. Pharmaceutics*, 2009, **6**, 1333–1342.
20 A. Akinc, M. Thomas, A. M. Klibanov and R. Langer, *J. Gene Med.*, 2005, **7**, 657–663.
21 T. A. Xia, M. Kovochich, M. Liong, H. Meng, S. Kabehie, S. George, J. I. Zink and A. E. Nel, *ACS Nano*, 2009, **3**, 3273–3286.
22 D. A. Wang, A. S. Narang, M. Kotb, A. O. Gaber, D. D. Miller, S. W. Kim and R. I. Mahato, *Biomacromolecules*, 2002, **3**, 1197–1207.
23 G. S. Manning, *Biophys. J.*, 2006, **91**, 3607–3616.
24 K. Besteman, K. Van Eijk and S. G. Lemay, *Nat. Phys.*, 2007, **3**, 641–644.
25 M. L. Ainalem and T. Nylander, *Soft Matter*, 2011, **7**, 4577–4594.
26 A. M. Carnerup, M. L. Ainalem, V. Alfredsson and T. Nylander, *Soft Matter*, 2011, **7**, 760–768.
27 A. M. Carnerup, M. L. Ainalem, V. Alfredsson and T. Nylander, *Langmuir*, 2009, **25**, 12466–12470.
28 K. Karim, J. D. Taylor, D. C. Cullen, M. J. Swann and N. J. Freeman, *Anal. Chem.*, 2007, **79**, 3023–3031.
29 A. Mashaghi, M. Swann, J. Popplewell, M. Textor and E. Reimhult, *Anal. Chem.*, 2008, **80**, 3666–3676.
30 G. H. Cross, A. Reeves, S. Brand, M. J. Swann, L. L. Peel, N. J. Freeman and J. R. Lu, *J. Phys. D: Appl. Phys.*, 2004, **37**, 74–80.
31 J. A. De Feijter, J. Benjamins and F. A. Veer, *Biopolymers*, 1978, **17**, 1759–1772.
32 L. Lee, A. P. R. Johnston and F. Caruso, *Biomacromolecules*, 2008, **9**, 3070–3078.
33 P. D. Coffey, M. J. Swann, T. A. Waigh, Q. S. Mu and J. R. Lu, *RSC Adv.*, 2013, **3**, 3316–3324.
34 J. Wang, X. W. Xu, Z. X. Zhang, F. Yang and X. R. Yang, *Anal. Chem.*, 2009, **81**, 4914–4921.
35 R. Deng, Y. Yue, F. Jin, Y. C. Chen, H. F. Kung, M. C. M. Lin and C. Wu, *J. Controlled Release*, 2009, **140**, 40–46.
36 R. Meszaros, L. Thompson, M. Bos and P. de Groot, *Langmuir*, 2002, **18**, 6164–6169.